Advances in Bioresearch
Adv. Biores., Vol 17 (1) January 2026: 16-34

Print ISSN 0976-4585; Online ISSN 2277-1573
Journal's URL:http://www.soeagra.com/abr.html
CODEN: ABRDC3
DOI: 10.15515/abr.0976-4585.17.1.1634

Advances in Bioresearch

ORIGINAL ARTICLE

Design, Optimization, and Evaluation of Prednisolone-Loaded Eudragit Nanosponges for Colon-Targeted Controlled Release Capsule Formulation

Shubhangi B. Khade*, Raosaheb S. Shendge
Department of Pharmaceutics, Sanjivani College of Pharmaceutical Education and Research, Savitribai Phule Pune University, Sahajanandnagar, Shingnapur, Kopargaon, Ahmednagar, Maharashtra 423603, India
Corresponding Author Email: Shubhangi.gite21@gmail.com

ABSTRACT
The present study aimed to develop and optimize nanosponges containing Prednisolone for colon-targeted drug delivery to enhance therapeutic efficacy and minimize systemic side effects. Nanosponges were prepared using the emulsion solvent evaporation method with Eudragit S-100 as the polymer and polyvinyl alcohol (PVA) as a stabilizer. A Central Composite Design (CCD) was applied to optimize the formulation by varying three independent variables—polymer concentration (X_1), surfactant concentration (X_2), and stirring speed (X_3)—to study their effect on particle size (Y_1), entrapment efficiency (Y_2), and cumulative drug release (Y_3). Among the twenty formulations, batch F11 (Eudragit S-100: 200 mg; PVA: 150 mg; 1000 rpm) exhibited optimal results with a mean particle size of 280.78 nm, entrapment efficiency of 83.24%, and cumulative drug release of 94.44% after 12 hours. FTIR, DSC, and XRD analyses confirmed drug–polymer compatibility and amorphous drug dispersion. SEM revealed uniform spherical morphology with smooth surfaces. The In Vitro release followed zero-order kinetics (R^2 = 0.9858) with a Higuchi diffusion-controlled mechanism. Capsules containing optimized nanosponges demonstrated sustained release up to 12 hours and remained stable under accelerated storage (40°C/75% RH) for 90 days. The developed nanosponge-based capsule formulation offers a promising platform for site-specific, controlled drug delivery of Prednisolone, providing a potential therapeutic advantage in the management of inflammatory bowel diseases and colonic disorders.
KEYWORDS: Prednisolone; Nanosponges; Eudragit S-100; Colon-targeted delivery; Controlled release; Central Composite Design (CCD)

Received 20.11.2025 Revised 01.12.2025 Accepted 31.12.2025

How to cite this article:
Shubhangi B. K, Raosaheb S. S. Design, Optimization, and Evaluation of Prednisolone-Loaded Eudragit Nanosponges for Colon-Targeted Controlled Release Capsule Formulation. Adv. Biores., Vol 17 (1) January 2026: 16-34.

INTRODUCTION

Targeted drug delivery systems have gained significant importance in recent years due to their ability to improve therapeutic efficacy, minimize systemic toxicity, and enhance patient compliance (1). Among these, colon-targeted delivery has emerged as a strategic approach for treating local diseases such as ulcerative colitis, Crohn's disease, and colorectal cancer, as well as for delivering drugs that are otherwise degraded or poorly absorbed in the upper gastrointestinal tract. Prednisolone, a potent glucocorticoid, is widely prescribed for inflammatory bowel diseases (IBD) due to its strong anti-inflammatory and immunosuppressive actions (2,3). However, its conventional oral administration is associated with poor bioavailability, rapid systemic clearance, and adverse systemic effects such as adrenal suppression and hyperglycemia. Therefore, developing a site-specific, controlled release system for Prednisolone targeting the colon is of immense therapeutic significance. Nanosponges have recently attracted attention as a novel drug delivery vehicle due to their porous structure, high surface area, and capability to encapsulate both hydrophilic and lipophilic drugs (4). These nanocarriers can control the drug release rate and improve solubility, stability, and bioavailability. Eudragit S-100, a pH-sensitive methacrylic acid copolymer, is particularly suitable for colon-targeted formulations as it remains intact in the acidic environment of the stomach and dissolves at pH above 7.0, corresponding to the intestinal milieu (5).

Polyvinyl alcohol (PVA) serves as a stabilizing agent to ensure uniform particle formation and prevent agglomeration during nanosponge preparation (6).

The Response Surface Methodology (RSM) using Central Composite Design (CCD) was employed to optimize the formulation variables systematically (7,8). This statistical tool provides a robust model for understanding the effects of independent variables and their interactions on key formulation parameters such as particle size, entrapment efficiency, and drug release. The emulsion solvent evaporation method was chosen for nanosponge synthesis due to its simplicity, reproducibility, and ability to produce uniform nanosized particles. The prepared nanosponges were extensively characterized for their physicochemical and morphological properties using techniques such as Fourier Transform Infrared Spectroscopy (FTIR), Differential Scanning Calorimetry (DSC), X-ray Diffraction (XRD), and Scanning Electron Microscopy (SEM). *In Vitro* release studies were conducted in phosphate buffer (pH 6.8) to simulate colonic conditions, and the release kinetics were analyzed using various mathematical models to determine the drug release mechanism (9,10). The optimized nanosponge batch was encapsulated into hard gelatin capsules to ensure dose uniformity and convenient administration.

This study aims to establish an effective nanosponge-based capsule formulation of Prednisolone that provides controlled, site-specific drug delivery to the colon. The successful development of such a formulation could significantly improve therapeutic outcomes in inflammatory bowel diseases by maintaining localized drug concentration, reducing dosing frequency, and minimizing systemic adverse effects.

MATERIAL AND METHODS

Drug Sample and Chemicals

The Prednisolone was acquired as a gift sample from Hetero Drugs, Hyderabad. Eudragit S-100 was procured as a gift sample from Lee Pharma Limited., Visakhapatnam, India. Solvents, Poly Vinyl Alcohol, and other chemicals (AR grade) were procured from SDFCL, Mumbai.

Identification and Confirmation of Drug

The identity and purity of the drug were confirmed through melting point determination, Fourier Transform Infrared (FTIR) spectroscopy (Shimadzu 8400S, Japan), and Differential Scanning Calorimetry (DSC, METTLER STAR SW 12.10). The melting point analysis provided the preliminary confirmation of the drug by comparing its characteristic melting behaviour, while FTIR spectroscopy was employed to identify the functional groups and verify the structural integrity of the compound. In addition, DSC was used to study the thermal behaviour and confirm the crystalline nature and purity of the drug. Together, these techniques ensured accurate identification and reliable confirmation of the drug (11).

UV Analysis of Prednisolone

10 µg/mL of Prednisolone solution was prepared by using methanol as solvent. The solution is scanned in (UV) spectrophotometer between 200 to 400 nm and the λ max was determined. This standard curve is used to estimate the concentration of the drug release from the formulation during the *In Vitro* dissolution studies (12,13).

Solubility Determination

The apparent solubility of Prednisolone was determined in methanol, water, and buffers pH 1.2, 6.8 at 37±0.5 °C. Excess of drug was added to 10 mL of solvent in glass vials with rubber closers, then the vials were kept on an orbital shaking incubator (Remi CIS-18; Remi Pvt. Ltd., India) maintained at 37±0.5 °C for 24 h. After shaking, the vials were kept in an incubator at 37±0.5 °C for equilibrium for 12 h. The solution was then filtered through 0.45 µm millipore filter and the filtrate was assayed by UV at λmax of 245 nm and the solubility was calculated by respective calibration curve (14).

Determination of drug-polymer compatibility

Drug–polymer compatibility was evaluated through both physical and chemical interaction studies using FTIR spectroscopy and DSC. FTIR was employed to compare the characteristic absorption spectra of the pure drug, excipients, and their physical mixtures, thereby identifying any possible chemical interactions or changes in functional groups. Similarly, DSC was performed to analyze the thermal behavior of the drug, excipients, and their blends, allowing assessment of any alterations in melting point, crystallinity, or thermal stability. Together, these techniques provided insights into the compatibility of the drug with selected excipients (15,16) .

Optimization by Factorial Design

A RSM-CCD (Response Surface Methodology-Central Composite Design) design was constructed where the X_1, X_2 and X_3 were selected as the three independent variables (17). It is suitable for investigating the quadratic response surfaces and for constructing a second-order polynomial model, thus enabling optimization. The levels of the three factors were selected on the basis of the preliminary studies carried

out before implementing the experimental design. All other formulation and processing variable were kept constant throughout the study. Optimization of nanosponges done by Design expert 13 statistical software trial packages, Stat-Ease 13.0.3.1. All the above formulations were prepared and evaluated for various parameters. The data was inputted to design expert software and polynomial equation was obtained. The responses (dependent variables) studied were Y_1, Y_2 and Y_3.

A RSM-CCD design was chosen for the optimization of Nanosponges because it allows the determination of influence of the factors with a minimum number of experiments. The independent factors were amount of Eudragit S-100 (X_1), amount of PVA (X_2) and swirling speed (X_3) for both factors. The response variables were Particle Size (nm) (Y_1), Entrapment Efficiency (%EE) (Y_2) and %Drug Release (Y_3) as shown in Table 1. 20 formulations were prepared according to factorial design. The formulations were F1 to F20. The responses obtained from the design matrix were statistically evaluated using Design expert 10 statistical software trial packages, Stat-Ease 13.0.3.1.

Table 1: Design Variables

Variables	Levels		
Independent	Eudragit S-100 (X_1) Levels: Low: 100mg and High: 200mg	PVA (X_2) Levels: Low: 50mg and High: 150mg	Swirling speed (X_3) Levels: Low: 500RPM and High: 1000RPM
Dependent	Particle Size (nm) (Y_1)	Entrapment Efficiency (%EE) (Y_2)	%Drug Release (Y_3)

Optimization data analysis and model-validation

ANOVA was used to establish the statistical validation of the polynomial equations generated by Design Expert® Software. Fitting a multiple linear regression model to a RSM design give a predictor equation incorporating interactive and polynomial term to evaluate the responses:

$$Y=\beta 0 +\beta 1\ X1 +\beta 2\ X2 +\beta 3\ X3 +\beta 12X12+\beta 22X22+\beta 1\ \beta 2\ X1\ X2 \text{---------- (1)}$$

Where Y is the measured response associated with each factor level combination; b_0 is an intercept representing the arithmetic average of all quantitative outcomes of nine runs; bi (b_1, b_2, b_{11}, b_{12} and b_{22}) are regression coefficients computed from the observed experimental values of Y and X_1 X_2 and X_3 are the coded levels of independent variables. The terms X_1 X_2 and X_3 represent the interaction terms. Three dimensional response surface plots resulting from equations were obtained by the Design Expert® software (15,17).

Preparation of PRED nanosponges

PRED nanosponges (F1-F20) were prepared using the emulsion solvent evaporation technique as shown in Table 2. Eudragit-S100 was employed as a polymer, and PVA was used as a surfactant in specified the choice of polymer and surfactant concentrations. First, the organic phase was produced by dissolving appropriate amounts of Eudragit-S100 and PRED in dichloromethane. PVA was dissolved in distilled water (100 ml) to prepare the aqueous phase. The two phases were combined by adding an organic phase drop-wise into the continuous aqueous phase and stirring for 2 hrs at 1000 rpm. The formed nanosponges were vacuum-filtered and dried at 40ºC for 24 hrs before being stored in a desiccator (18,19).

Table 2: Formulations Batches as per RSM-CCD design

Formulation Code	Prednisolone (mg)	Eudragit S-100 (mg)	PVA (mg)	Swirling speed (RPM)
F1	40mg	150	100	1170.45
F2		150	100	750
F3		150	100	329.552
F4		234.09	100	750
F5		150	100	750
F6		100	150	1000
F7		150	100	750
F8		100	150	500
F9		150	184.09	750
F10		100	50	500
F11		200	150	1000
F12		200	50	1000
F13		150	100	750
F14		150	100	750
F15		200	50	500
F16		100	50	1000
F17		200	150	500
F18		65.9104	100	750
F19		150	15.9104	750
F20		150	100	750

Evaluation of optimized nanosponges formulation

Particle size, Zeta potential, and Polydispersity Index (PDI)

Zetasizer (Malvern Nano ZS) was used to determine the average particle size, PDI, and surface charge of formulation dissolved in distilled water was added to each sample for dilution before analysis and analyzed at 25±0.5 ^{0}C.

% EE and drug loading capacity (%DL)

The percentage of drug entrapped inside the nanosponge formulation is referred to as %EE. To determine the %DL and %EE, 50 mg of nanosponges was dissolved in 10 mL of phosphate buffer (pH 6.8), and the sample was agitated until complete dissolution (20–22). The resulting transparent drug layer was collected for analysis. The amount of PRED in the nanosponges was evaluated utilizing a UV-visible spectrophotometer, and the %EE of the PRED was calculated:

%EE=Total amount of drug-Free drug in solution/Total amount of drug X 100 ----- (2)

%DL= Total amount of drug-Free drug in solution/Total amount of nanosponge X 100 --- (3)

XRD analysis

The X-ray diffraction pattern of selected batches of nanosponges was carried out using X'-Pert Model, Phillips to characterize the physical form of Prednisolone. The data was recorded at 2θ within 0–90° of the range inside copper target tube of X-ray at the step size of 0.0500.

DSC analysis

The thermal behaviour of the samples was studied by Differential Scanning calorimeter (DSC-PYRIS-1, perkin elmer). DSC scan was carried out in an atmosphere of dry nitrogen within the measuring range of -2-20MW. The samples were heated at a rate of 10°C min^{-1} from room temperature to the melting point using reference of an empty aluminum pan (23).

SEM Analysis

The PRED was morphologically characterized using scanning electron microscope (Carl Zeiss SEM with Oxford EDX) in a high vacuum mode (24).

***In-vitro* drug release study**

The *in-vitro* dissolving apparatus USP-II (paddle method, Labtronics dissolution apparatus) was used to estimate the drug release within a temperature range of 37±0.2ºC. Phosphate buffer of 900 mL at a pH 6.8 and100 rpm was used. Nanosponges, equivalent to 40 mg of the drug, were measured, packed into a diffusion sachet, and placed into a dissolution beaker for drug dissolution testing. UV-VIS spectral analysis at 245nm evaluated the drug's concentration after samples were taken at specific intervals ranging from 1 to 12 hr. The release pattern of RF's medication was examined by fitting the results of each dissolving sample into the most appropriate kinetic models (25).

Preformulation studies of Nanosponges and Pure Drug

Flow properties such as angle of repose, bulk density, tapped density and compressibility index of optimized formulations, and were evaluated to determine the suitability for capsule formulation

Formulation of Capsule using optimized nanosponges

Prednisolone Nanosponges were formulated by emulsion solvent evaporation method using Eudragit S-100 as a polymer, PVA as a stabilizer/surfactant and finally enclosed in hard gelatin Capsules.

Evaluation of Prednisolone Nanosponges Capsules

Uniformity of weight

Intact capsule was weighed. The capsules (Size Zero) were opened without losing any part of the shell and contents were removed as completely as possible. The shell was washed with ether and the shell allowed to stand until the odor of the solvent was no longer detectable. The empty shell was weighed. The average weight was determined. Not more than two of the individual weights deviate from the average weight by more than the percentage deviation and none deviates by more than twice that percentage.

Drug content

Five capsules were selected randomly and the average weight was calculated. An amount of powder was equivalent to 40 mg of Prednisolone was made upto 100 ml with phosphate buffer pH 6.8. It was kept overnight. 1 ml of solution was diluted to 50 ml using phosphate buffer pH 6.8 in separate standard flask. The absorbance of solution was recorded at 245 nm.

***In-vitro* drug release study**

The *in-vitro* drug release study was conducted using the USP-II (paddle method) dissolution apparatus (Labtronics). The study was performed at a controlled temperature of 37±0.2°C using 900 mL of phosphate buffer (pH 6.8) as the dissolution medium. The paddle rotation speed was maintained at 100 rpm. Capsules, containing nanosponges equivalent to 40 mg of the drug, were introduced into the dissolution medium. At predetermined time intervals (ranging from 1 to 12 hours), aliquots were withdrawn, and the same volume was replaced with fresh dissolution medium to maintain sink

conditions. The withdrawn samples were filtered and analyzed for drug concentration using UV-Visible spectrophotometry at 245 nm. The drug release data were analyzed to determine the release kinetics by fitting the results into various kinetic models, such as zero-order, first-order, Higuchi, and Korsmeyer-Peppas models, to identify the most suitable release mechanism (26).

Kinetics of Drug Release

Drug release from pharmaceutical dosage forms follows distinct kinetic patterns that can be characterized by mathematical models. Zero-order kinetics describes systems that release a constant amount of drug per unit time, commonly observed in transdermal systems and matrix capsules containing poorly soluble drugs. First-order kinetics characterizes drug release proportional to the remaining drug amount, resulting in decreasing release rates over time as the drug reservoir depletes. The Higuchi model specifically addresses diffusion-controlled release mechanisms for both water-soluble and poorly water-soluble drugs in semi-solid and solid matrices, where drug release is proportional to the square root of time. Finally, the Korsmeyer-Peppas model provides a comprehensive approach to characterize different release mechanisms through the analysis of the relationship between cumulative drug release and time, with the slope parameter (n) indicating the specific type of release mechanism governing the system.

Stability studies

The stability of Prednisolone nanosponges capsule was monitored up to 90 days at ambient temperature and relative humidity (40°C/75%RH). Periodically samples were withdrawn and characterized by Physical Appearance, Drug Content and Dissolution.

RESULT AND DISCUSSION

Melting Point Determination of Prednisolone

The melting point of Prednisolone was determined using the capillary method. The observed melting point of Prednisolone was confirmed with standard melting point of Prednisolone as shown in Table 3.

Table 3: Melting Point of Prednisolone

Trial	Observed Melting Point (°C)
1	235–237 ^{0}C
2	236–237 ^{0}C
3	237–239 ^{0}C
Mean	236.83 ^{0}C

FTIR

The FTIR spectrum of Prednisolone exhibits characteristic absorption bands confirming its functional groups. A broad O-H stretching band appears at 3420 cm^{-1}, while C-H stretching vibrations are observed at 2930 cm^{-1}. The strong C=O stretching peak at 1705 cm^{-1} indicates the presence of ketone groups, and C=C stretching occurs at 1625 cm^{-1}. The C-O stretching band at 1080 cm^{-1} confirms ester or ether functionalities, while CH_2 and CH_3 bending vibrations at 1380–1450 cm^{-1} further validate the steroidal structure. These peaks confirm the presence of hydroxyl, ketone, alkene, ester, and alkyl groups in Prednisolone as shown in Figure 3.

Differential Scanning Calorimetry

DSC analysis of Prednisolone performed at a 10 ºC/min of scanning rate with continuous nitrogen splurging revealed a sharp endothermic peak at 225.77ºC (Figure 4), confirms with the specified melting point range of 225-238 ºC.

UV-Visible spectrophotometer

The Prednisolone solution was subjected to scanning from 400 nm to 200 nm, and it exhibited peak absorption at 245 nm, as depicted in Figure 1. This observation was in agreement with the previously documented and published UV-Visible spectrum of Prednisolone, which also indicated a maximum absorption at 245 nm (λ max).

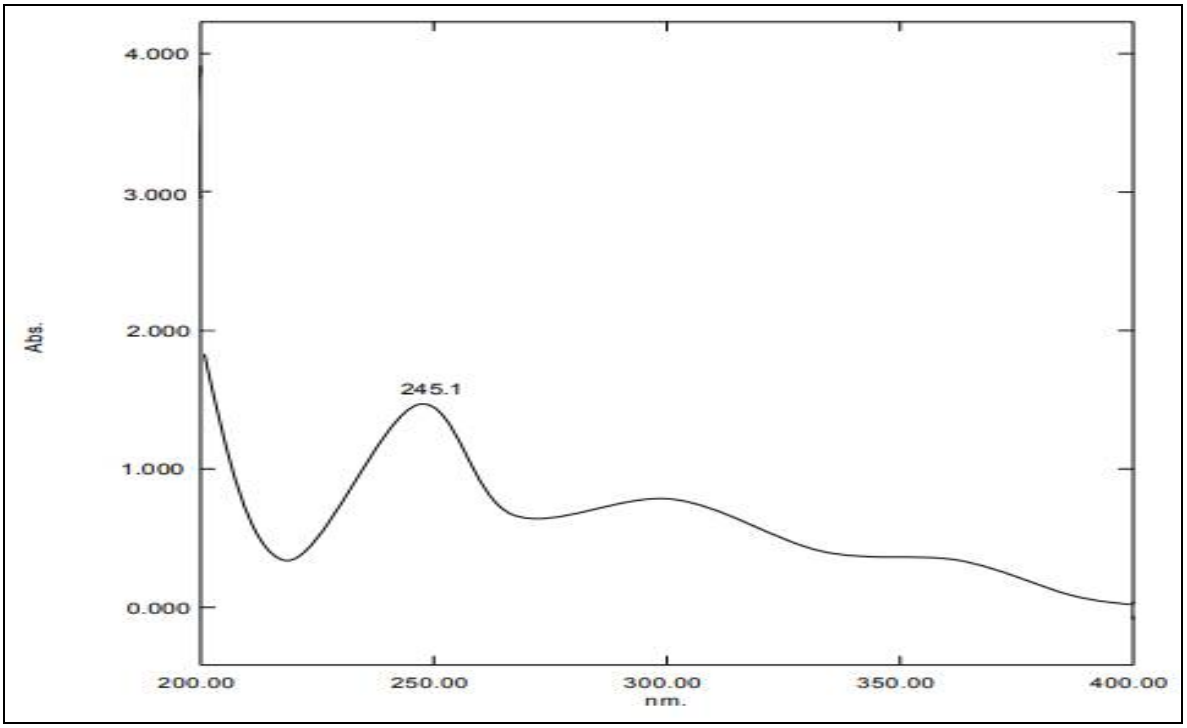

FFigure 1: UV spectrum of Prednisolone

Solubility study of drug in diverse solvent

The solubility of Prednisolone as a function of pH is illustrated in Table 4 and illustrated in Figure 2. The solubility profile suggests that the compound is poorly soluble in water but exhibits significantly higher solubility in methanol and phosphate buffer at pH 6.8. This information is crucial for formulating the compound for biological studies or pharmaceutical applications, as choosing an appropriate solvent can enhance bioavailability and efficacy. The high solubility in phosphate buffer also suggests that the compound could have favorable solubility in biological fluids, which is advantageous for *in-vitro* studies.

Table 4: Solubility data of Prednisolone

Medium	Solubility (mg/ml)
Distilled Water	0.084±0.0015
Methanol	7.24±0.065
Phosphate buffer pH 1.2	0.0026±0.0008
Phosphate buffer pH 6.8	9.66±0.09

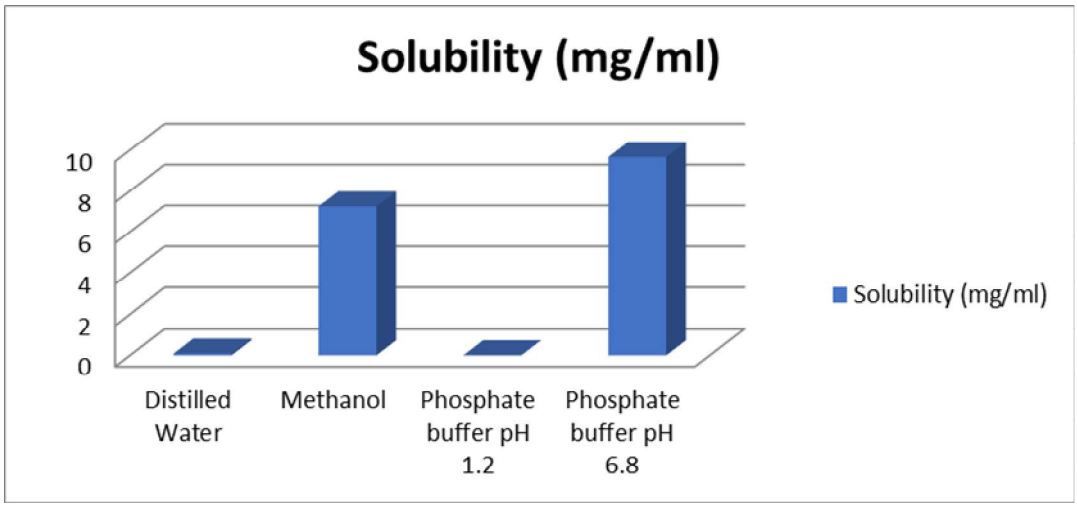

Figure 2: Solubility Study Data

Determination of drug-polymer compatibility

FTIR

The drug-excipients compatibility study is crucial for confirming the identity of the product and ensuring its reproducibility with guaranteed therapeutic efficacy. This method was used to identify any interactions between Prednisolone and Eudragit S-100 PVA, as well as their physical mixtures. The spectra of Prednisolone, Eudragit S-100, PVA and the physical mixtures are shown in Figures 3. A broad O-H stretching band appears at 3420 cm^{-1}, while C-H stretching vibrations are observed at 2930 cm^{-1}. The strong C=O stretching peak at 1705 cm^{-1} indicates the presence of ketone groups, and C=C stretching occurs at 1625 cm^{-1}. The C-O stretching band at 1080 cm^{-1} confirms ester or ether functionalities, while CH_2 and CH_3 bending vibrations at 1380–1450 cm^{-1} further validate the steroidal structure. These peaks confirm the presence of hydroxyl, ketone, alkene, ester, and alkyl groups in Prednisolone. The FTIR spectra of the physical mixture showed similar results to the pure drug, indicating no interaction and confirming compatibility.

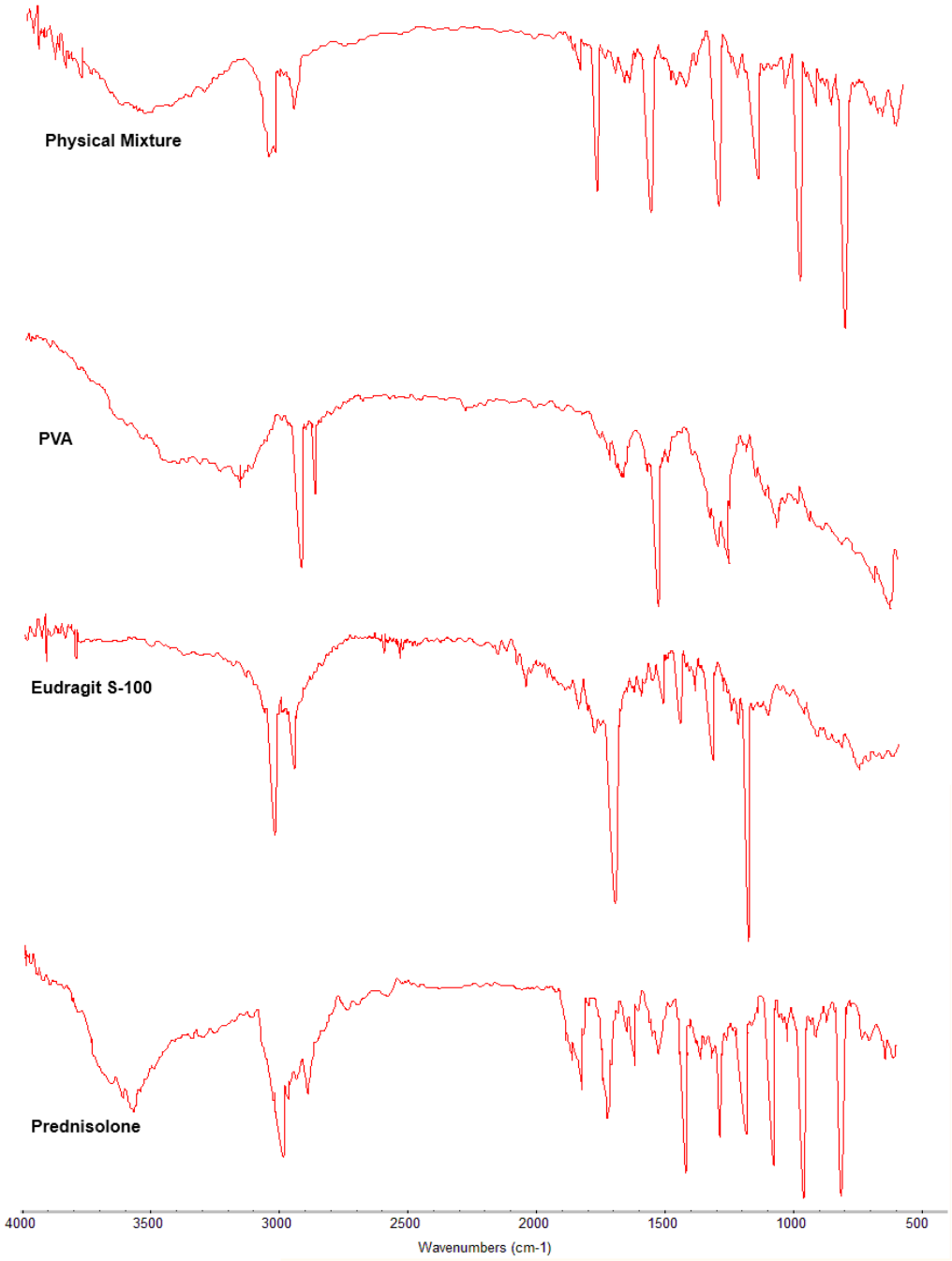

Figure 3: FTIR spectra of Prednisolone, Eudragit S-100, PVA and Physical Mixture

Differential Scanning Calorimetry

The drug's melting point was determined using Differential Scanning Calorimetry (DSC). Thermograms for the pure drug Prednisolone, Eudragit S-100, PVA, and their physical mixtures were obtained using the Mettler DSC 1-star system (Mettler-Toledo, Switzerland). The samples, placed in perforated aluminum pans, were heated at a constant rate of 10°C/min within a temperature range of 30-300°C, as shown in Figures 4. DSC analysis of Prednisolone, conducted at a scanning rate of 10ºC/min with continuous nitrogen flow, revealed a sharp endothermic peak at 225.77ºC, which aligns with the specified melting point range of 225-235ºC. Eudragit S-100 showed a sharp endothermic peak at 162.78ºC, consistent with its specified melting point range of 150-210ºC. PVA showed a sharp endothermic peak at 224.76ºC, consistent with its specified melting point range of 200-250ºC. The thermogram of the physical mixture displayed similar results to the pure drug, Eudragit S-100 and PVA, indicating no interaction and confirming compatibility.

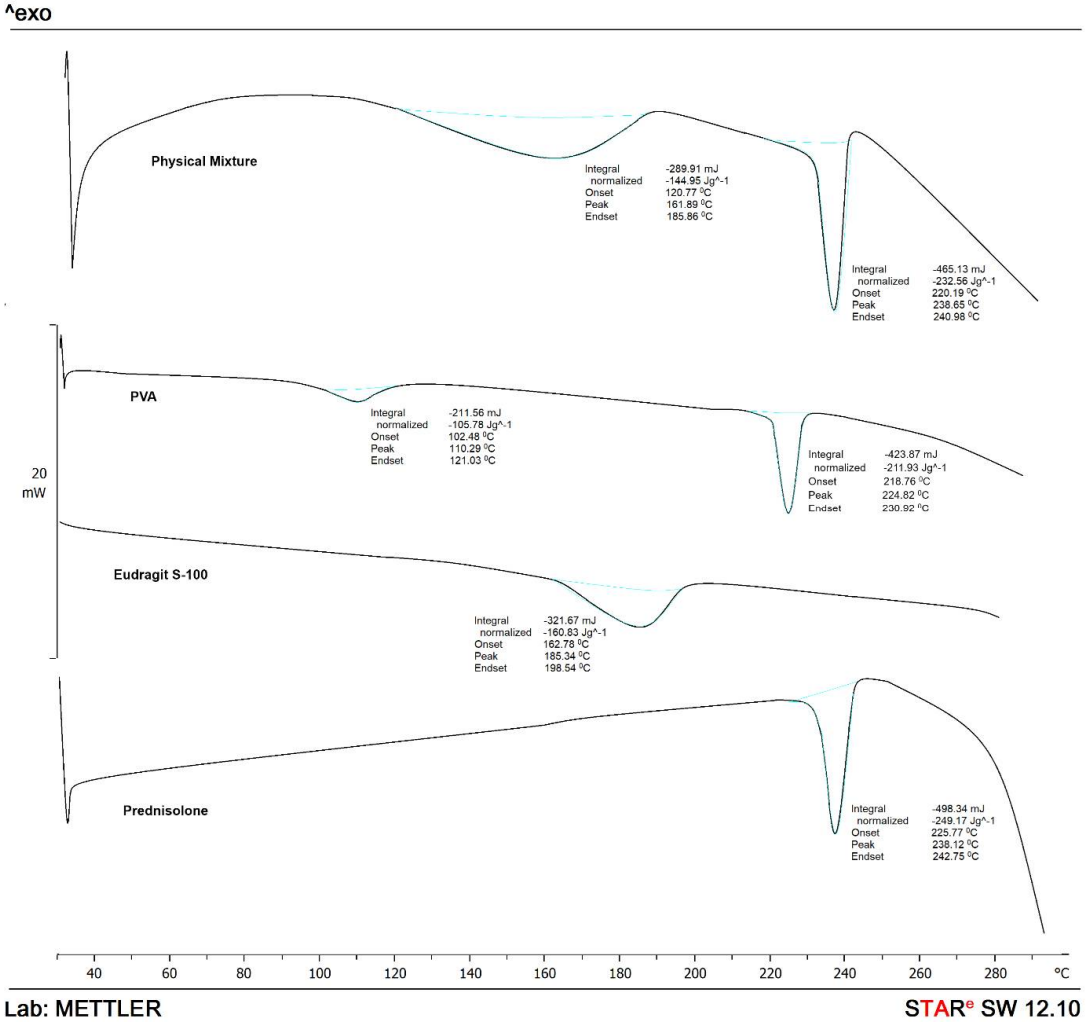

Figure 4: DSC graph of Prednisolone, Eudragit S-100, PVA and Physical Mixture

Formulation Design

Various Formulation batches of nanosponges were prepared by based on RSM factorial designs. The independent variables were amount of Eudragit S-100 (X_1), amount of PVA (X_2) and swirling speed (X_3) for factors and their levels are shown in table 5 particle size (nm) (Y_1) and Entrapment Efficiency (%EE) (Y_2), and %Drug Release (Y_3) were taken as response parameters as the dependent variables.

Table 5: Design Batches

Formulation Code	X_1 (mg)	X_2 (mg)	X_3 (RPM)	Y_1 (nm)	Y_2 (%)	Y_3 (%)
F1	150	100	1170.45	289.88	82.94	93.2
F2	150	100	750	353.05	82.51	91.85
F3	150	100	329.552	349.8	82.49	92
F4	234.09	100	750	357.29	83.4	91.74
F5	150	100	750	353.05	82.51	91.85
F6	100	150	1000	287.07	83.83	93.23
F7	150	100	750	353.05	82.51	91.85
F8	100	150	500	337.71	82.44	92.39
F9	150	184.09	750	300.39	82.72	93.22
F10	100	50	500	287.88	83.79	93.01
F11	**200**	**150**	**1000**	**280.78**	**83.24**	**94.44**
F12	200	50	1000	301.95	82.93	93.14
F13	150	100	750	353.05	82.51	91.85
F14	150	100	750	353.05	82.51	91.85
F15	200	50	500	322.59	83.78	92.55
F16	100	50	1000	321.75	83.4	90.56
F17	200	150	500	385.91	82.31	90.31
F18	65.9104	100	750	333.4	83.9	91.32
F19	150	15.9104	750	276.3	83.59	92.86
F20	150	100	750	353.05	82.51	91.85

Optimization data analysis and model-validation

A) Fitting of data to model:

The three factors with lower, middle and upper design points in coded and un-coded values are shown in below tables. All the responses observed for 20 formulations prepared were fitted to Quadratic effect model, which was found as the best fitted model for Y_1, Y_2, and Y_3, using Design Expert® software. The values of R^2, adjusted R^2, predicted R^2, SD and % CV are given in (Table 12), along with the regression equation generated for each response. The results of ANNOVA in (Table 6), for the dependent variables demonstrate that the model was significant for all the response variables. It was observed that independent variables X_1 (mg), X_2 (mg) and X_3 (RPM) had a positive effect on the nanosponges.

Table 6: Summary of results of regression analysis for responses Y_1, Y_2, and Y_3

Models	R^2	Adjusted R^2	Predicted R^2	SD	%CV
Response (Y_1) Quadratic Effect	1.000	1.000	1.000	0.0033	0.0010
Response (Y_2) Quadratic Effect	1.000	1.000	1.000	0.0015	0.0018
Response (Y_3) Quadratic Effect	1.000	1.000	1.000	0.0016	0.0018

Regression Equations:

$Y1=353.05+7.10A+7.16B-17.82C+3.375AB-13.625AC-21.125BC-2.72A^2-22.88B^2-11.74C^2$---------- (13)

$Y2=82.51-0.149A-0.259B+0.134C-0.03AB-0.115AC+0.445BC+0.403A^2+0.228B^2+0.073C^2$---------- (14)

$Y3=91.85+0.124A+0.107B+0.356C-0.406AB+0.759AC+0.821BC-0.113A^2+0.420B^2+0.265C^2$---------- (15)

The polynomial regression equations Y_1, Y_2, and Y_3 describe the relationships between the dependent variables (Y_1, Y_2, and Y_3) and the independent variables (A, B and C), including their linear, interaction (ABC), and quadratic effects. These equations demonstrate how changes in A, B and C, individually and in combination, influence Y_1, Y_2, and Y_3, with quadratic terms accounting for non-linear variations.

B) Model Assessment for Dependent Variables:

After putting the data in Design Expert® software for, Fit summary applied to data in that Quadratic Effect Model had been suggested by the software for all the responses. The statistical evaluation was performed by using ANNOVA. Results are shown in (Table 7, 8 and 9). The coefficients with more than one factor term in the regression equation represent interaction terms. It also shows that the relationship between

factors and responses is not always linear. When more than one factor are changes simultaneously and used at different levels in a formulation, a factor can produce different degrees of responses.

Table 7: Results of Analysis of Variance for Measured Response

Source	Sum of Squares	df	Mean Square	F-value	p-value	
Model	19721.00	9	2191.22	2.040E+08	< 0.0001	significant
A-Eudragit S-100	688.93	1	688.93	6.414E+07	< 0.0001	
B-PVA	700.58	1	700.58	6.522E+07	< 0.0001	
C-Swirling speed	4334.91	1	4334.91	4.036E+08	< 0.0001	
AB	91.13	1	91.13	8.483E+06	< 0.0001	
AC	1485.13	1	1485.13	1.383E+08	< 0.0001	
BC	3570.12	1	3570.12	3.324E+08	< 0.0001	
A^2	106.99	1	106.99	9.960E+06	< 0.0001	
B^2	7542.41	1	7542.41	7.022E+08	< 0.0001	
C^2	1986.98	1	1986.98	1.850E+08	< 0.0001	
Residual	0.0001	10	0.0000			
Lack of Fit	0.0001	5	0.0000			
Pure Error	0.0000	5	0.0000			
Cor Total	19721.00	19				

Table 8: Results of Analysis of Variance for Measured Response

Source	Sum of Squares	df	Mean Square	F-value	p-value	
Model	6.03	9	0.6703	2.858E+05	< 0.0001	significant
A-Eudragit S-100	0.3050	1	0.3050	1.300E+05	< 0.0001	
B-PVA	0.9192	1	0.9192	3.920E+05	< 0.0001	
C-Swirling speed	0.2470	1	0.2470	1.053E+05	< 0.0001	
AB	0.0072	1	0.0072	3070.03	< 0.0001	
AC	0.1058	1	0.1058	45112.36	< 0.0001	
BC	1.58	1	1.58	6.755E+05	< 0.0001	
A^2	2.34	1	2.34	9.997E+05	< 0.0001	
B^2	0.7514	1	0.7514	3.204E+05	< 0.0001	
C^2	0.0763	1	0.0763	32548.89	< 0.0001	
Residual	0.0000	10	2.345E-06			
Lack of Fit	0.0000	5	4.691E-06			
Pure Error	0.0000	5	0.0000			
Cor Total	6.03	19				

Table 9: Results of Analysis of Variance for Measured Response

Source	Sum of Squares	df	Mean Square	F-value	p-value	
Model	17.15	9	1.91	7.119E+05	< 0.0001	significant
A-Eudragit S-100	0.2107	1	0.2107	78742.96	< 0.0001	
B-PVA	0.1551	1	0.1551	57965.71	< 0.0001	
C-Swirling speed	1.74	1	1.74	6.485E+05	< 0.0001	
AB	1.32	1	1.32	4.934E+05	< 0.0001	
AC	4.61	1	4.61	1.721E+06	< 0.0001	
BC	5.40	1	5.40	2.016E+06	< 0.0001	
A^2	0.1855	1	0.1855	69323.43	< 0.0001	
B^2	2.55	1	2.55	9.519E+05	< 0.0001	
C^2	1.01	1	1.01	3.778E+05	< 0.0001	
Residual	0.0000	10	2.676E-06			
Lack of Fit	0.0000	5	5.352E-06			
Pure Error	0.0000	5	0.0000			
Cor Total	17.15	19				

C) Response Surface Plot Analysis

Three-dimensional response surface plots were generated by the Design Expert® software are presented in Figure 5 (A&B); Figure 6 (A&B) and Figure 7 (A&B) for the studied responses, i.e. Particle size (nm) (Y_1), Entrapment Efficiency (%EE) (Y_2) and %Drug Release (Y_3). Figure 5 depicts response surface plot of Eudragit S-100 concentration (X_1), PVA (X_2) and swirling speed (X_3) on particle size (Y_1). Nanosponges being formulation batch amongst all the design batches giving optimum particle size will be preferred

more and selected as an optimized batch. The smallest particle size was observed in F11 (280.78 nm), which contained coded concentrations of X_1, X_2 and X_3. This indicates that a balanced concentration of X_1, X_2 and X_3 might result in more stable particle formation, minimizing aggregation and producing smaller particles. The results suggest that an optimal ratio of X_1, X_2 and $X_3$is crucial for controlling particle size.

Figure 5 depicts response surface plot of Eudragit S-100 concentration (X_1) and PVA (X_2) (%EE) (Y_2) and %CDR (Y_3). To determine the optimized batch, we need to balance high entrapment efficiency (%EE), desirable particle size (Y1), and high cumulative drug release (%CDR). Among all formulations, F6 (83.83%), F10 (83.79%), and F18 (83.9%) had the highest EE, while F11 (280.78 nm), F19 (276.3 nm), and F10 (287.88 nm) exhibited the smallest particle sizes, and F11 (94.18%), F6 (93.23%), and F9 (93.22%) showed the highest %CDR. Based on these factors, Batch F11 (X1 = 200 mg, X2 = 150 mg, X3 = 1000 RPM) was identified as the optimized formulation due to its superior balance of high EE (83.24%), smallest particle size (280.78 nm), and highest drug release (94.18%), making it ideal for effective drug delivery and absorption.

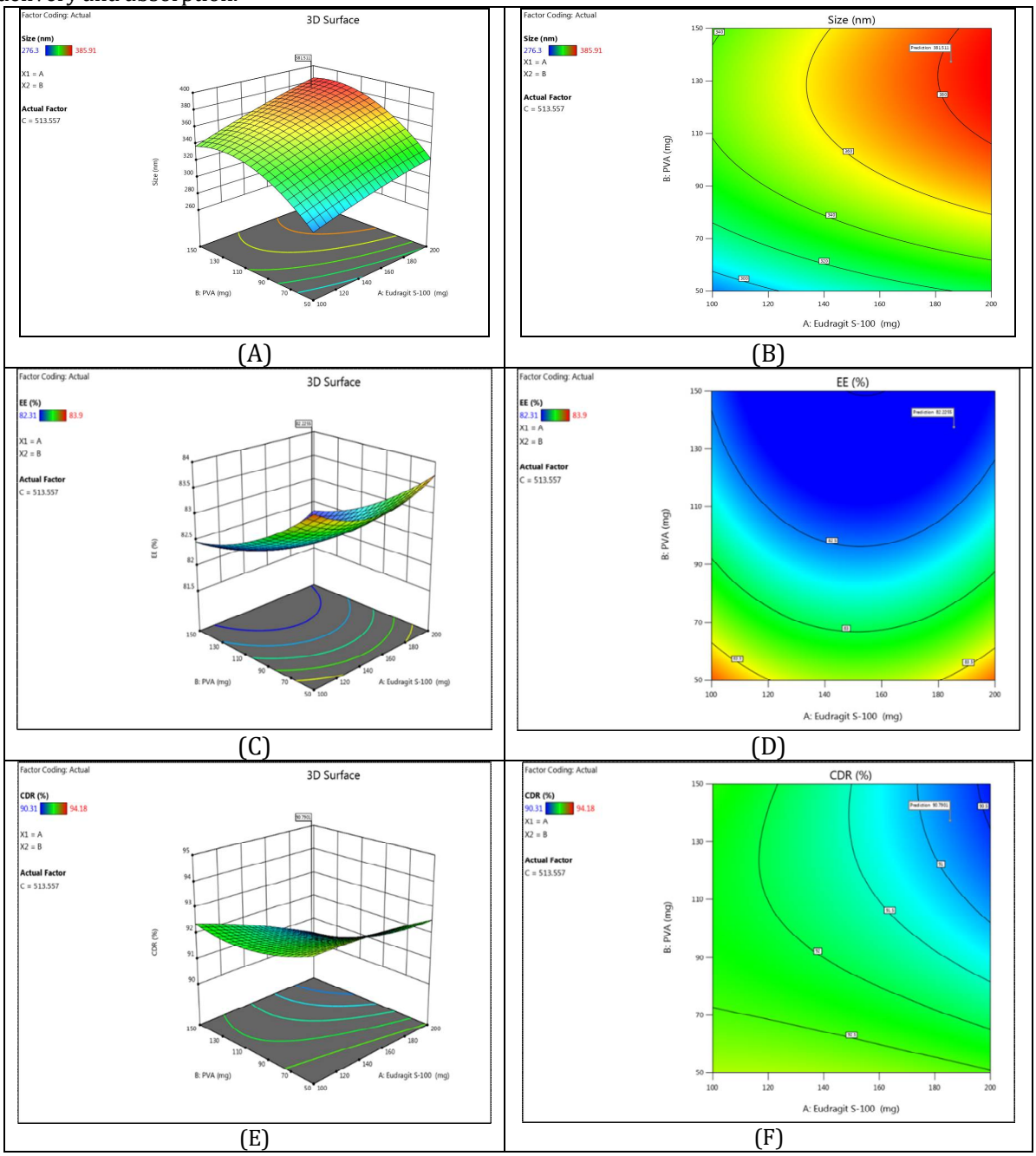

Figure 5. 3D surface plots (A) Particle size (nm); (C) EE (%); (E) CDR (%); Contour Plots (B) Particle size (nm); (D) EE (%); (F) CDR (%)

The Quadratic model demonstrates significant results with a p-value less than 0.05. The ANOVA test was conducted, and the results were significant.

Evaluation of optimized nanosponges formulation

Particle size, Zeta potential, and Polydispersity Index (PDI)

The optimal formulation F11 contained particles that were nanosized and maintained in separation by repulsive forces, as shown in Figure 6 and 7. The average particle size was 280.78nm, the zeta potential was -28.8mV, and the PDI was 0.189.

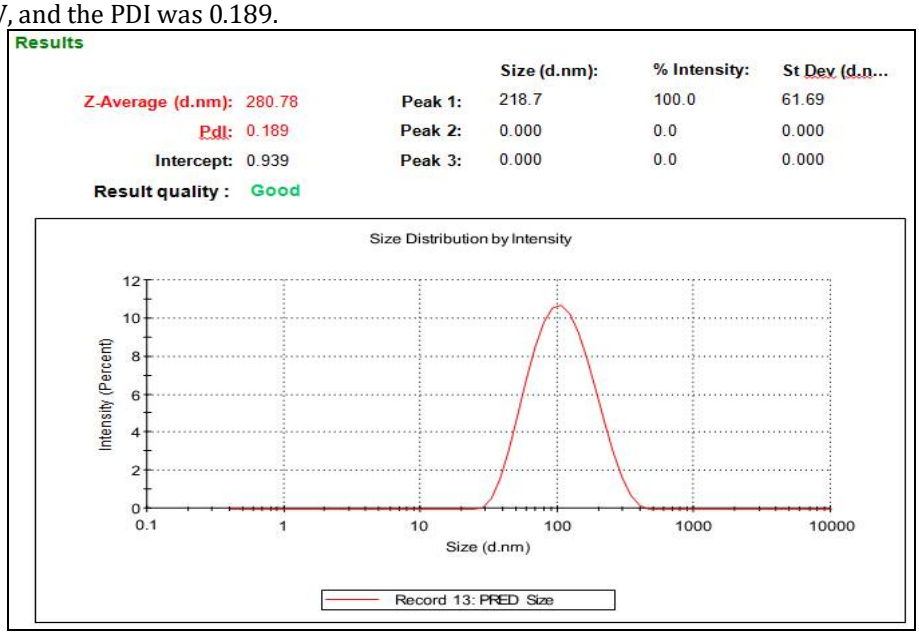

Figure 6: Particle size of F11 batch

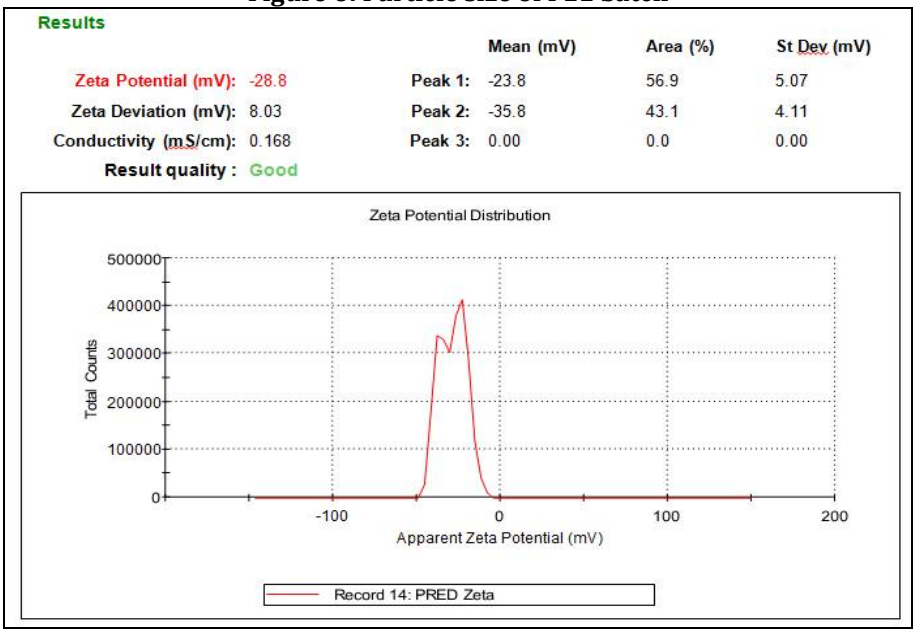

Figure 7: Zeta Potential of F11 batch

% EE and drug loading capacity (%DL)

The drug %EE and %DL capacity of all the nanosponges (F1-F20) were observed between 82.51±0.13 to 84.90±0.28% and 70.80±0.20 to 80.32±0.20%, respectively, and are shown in Table 10.

Table 10: % EE and %DL of batches

Batch Code	%EE (Mean ± SD)	DL (Mean ± SD)
F1	82.94 ± 0.11	71.51 ± 0.10
F2	82.51 ± 0.12	79.92 ± 0.12
F3	82.49 ± 0.13	79.61 ± 0.14
F4	83.40 ± 0.14	80.25 ± 0.16
F5	82.51 ± 0.15	79.32 ± 0.18
F6	83.83 ± 0.16	80.32 ± 0.20
F7	82.51 ± 0.17	77.32 ± 0.09
F8	82.44 ± 0.18	74.11 ± 0.11
F9	82.72 ± 0.19	72.53 ± 0.13
F10	83.79 ± 0.20	73.21 ± 0.15
F11	**83.24 ± 0.21**	**72.31 ± 0.17**
F12	82.93 ± 0.22	70.93 ± 0.19
F13	82.51 ± 0.23	71.11 ± 0.21
F14	82.51 ± 0.24	71.20 ± 0.22
F15	83.78 ± 0.25	72.50 ± 0.23
F16	83.40 ± 0.26	73.10 ± 0.24
F17	82.31 ± 0.27	70.80 ± 0.20
F18	83.90 ± 0.28	73.50 ± 0.25
F19	83.59 ± 0.29	73.00 ± 0.21
F20	82.51 ± 0.30	71.30 ± 0.22

XRD analysis

The confirmation of the formation of PRED nanosponges was illustrated in Figure 8 by observing a smoother XRD curve for the PRED nanosponges relative to a purified substance.

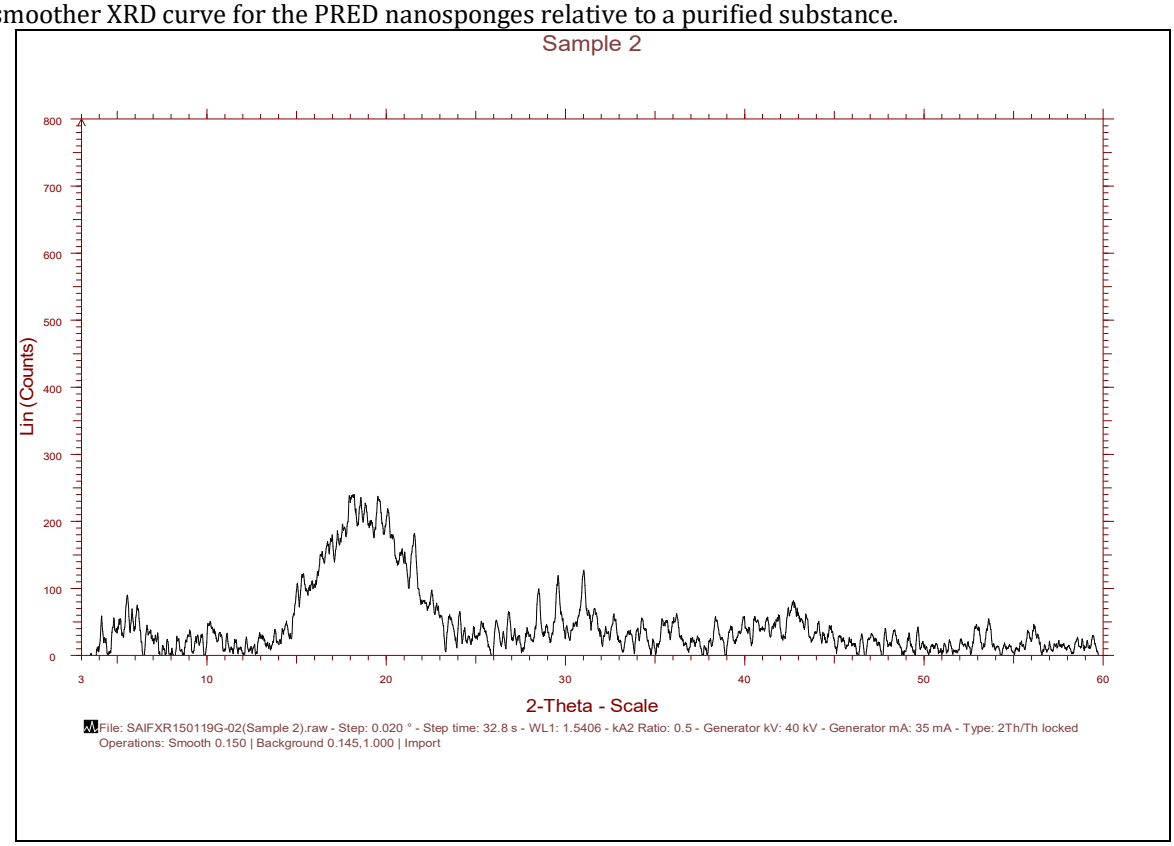

Figure 8: XRD of F11 batch

DSC analysis

An endothermic peak for melting was observed at 225.77ºC on the DSC thermogram of the PRED pure substance. The nanosponges of Prednisolone in the amorphous nanosponge core is indicated in Figure 9, as the endothermic peak of the nanosponge was 229.47ºC, which is in closer proximity to the 225.77ºC peak of ES100.

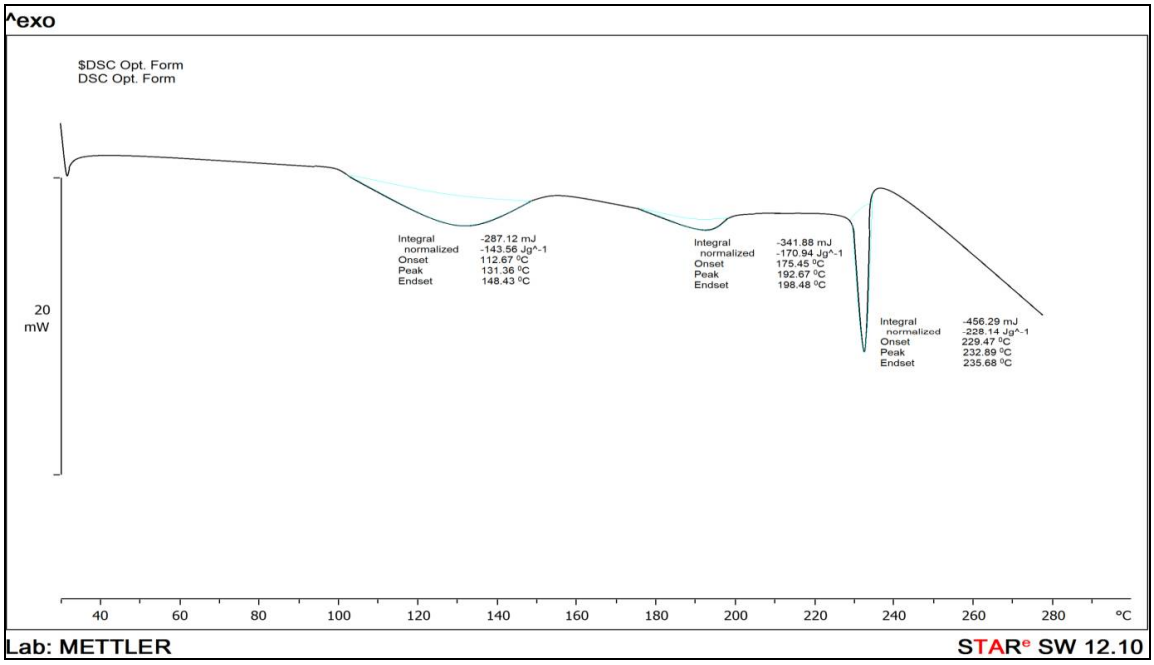

Figure 9: DSC of F11 batch

SEM Analysis

As per the SEM analysis, the nanosponge Formulation (F1-F20) achieved particle size ranging from 276-385nm (Table 11). As shown in Figure 10, the nanosponge surface had no trace of any crystalline drug particles, and the particle diameters of all formulations remained constant.

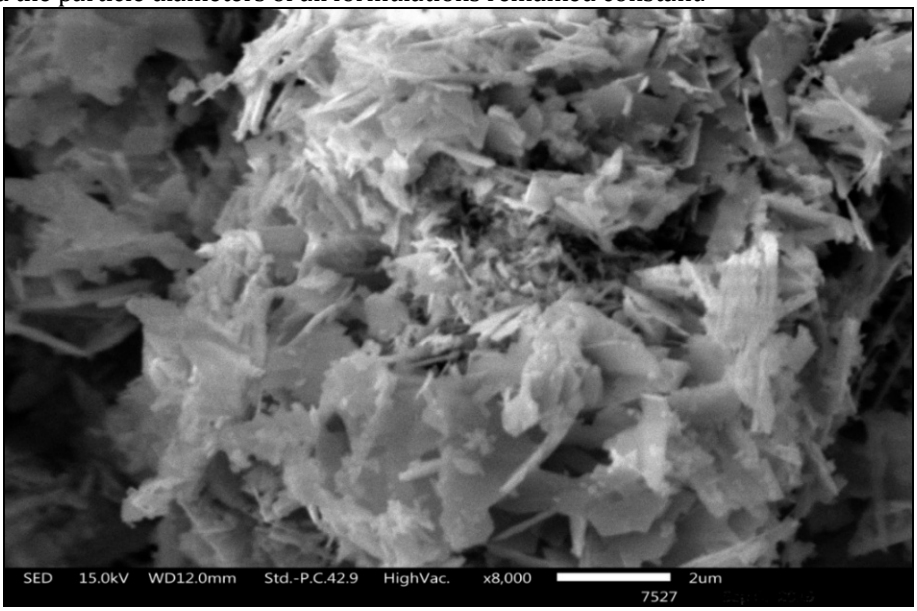

Figure 10: SEM image of F11 batch

***In-vitro* drug release study**

The PRED nanosponges (F11) dissolution study was conducted using a USP-II dissolution apparatus at 37±0.5ºC with 100 rpm using phosphate buffer (pH-6.8). Samples were collected at 0, 2, 4, 6, 8, 10 and 12 hrs. Drug release rates for all formulations ranged from 90.31±0.30% to 94.18±0.32% within 12 hrs as shown in Table 11 & 12 and Figure 11.

Table 11: *In-vitro* release profile of all batches of nanosponges

Batch Code	%CDR (Mean ± SD)
F1	93.20 ± 0.27
F2	91.85 ± 0.25
F3	92.00 ± 0.26
F4	91.74 ± 0.28
F5	91.85 ± 0.24
F6	93.23 ± 0.29
F7	91.85 ± 0.23
F8	92.39 ± 0.30
F9	93.22 ± 0.27
F10	93.01 ± 0.31
F11	**94.44 ± 0.32**
F12	93.14 ± 0.26
F13	91.85 ± 0.28
F14	91.85 ± 0.25
F15	92.55 ± 0.29
F16	90.56 ± 0.27
F17	90.31 ± 0.30
F18	91.32 ± 0.28
F19	92.86 ± 0.26
F20	91.85 ± 0.31

Table 12: *In-vitro* release profile of optimized nanosponges

Sr. No.	Time (Hours)	F11
1	0	0
2	2	28.61±0.04
3	4	58.17±0.03
4	6	62.82±0.02
5	8	66.62±0.09
6	10	82.18±0.03
7	12	94.44±0.01

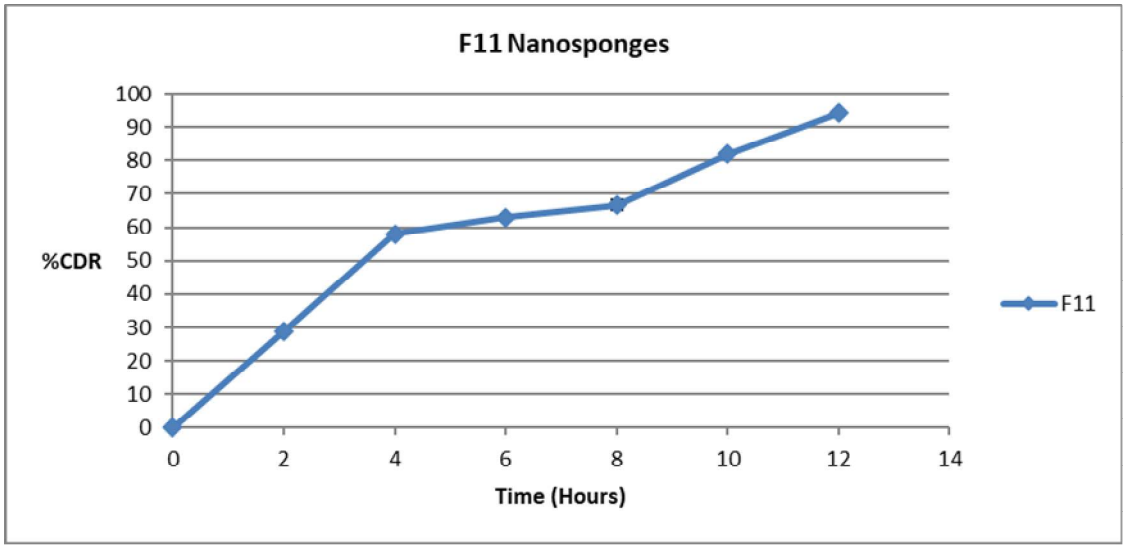

Figure 11: *In-vitro* drug release of nanosponges (F11)

Preformulation studies of Nanosponges

Flow properties such as angle of repose, bulk density, tapped density and compressibility index of optimized formulations, and were evaluated to determine the suitability for nanosponges formulation. F11 optimized batch show good flow proprieties and other batches show fair flow properties as shown in Table 13.

Table 13: Pre-Compression Parameters of Nanosponges

Batch Code	Bulk Density (gm/ml)	Tapped Density (gm/ml)	Carr's Index (%)	Hausner Ratio	Angle of Repose
F1	0.55 ± 0.03	0.52 ± 0.03	19.11 ± 0.02	1.14 ± 0.03	23.42 ± 0.11
F2	0.47 ± 0.03	0.55 ± 0.03	16.29 ± 0.02	1.17 ± 0.03	24.58 ± 0.23
F3	0.53 ± 0.02	0.67 ± 0.03	18.52 ± 0.02	1.25 ± 0.03	24.40 ± 0.21
F4	0.52 ± 0.03	0.63 ± 0.02	19.11 ± 0.03	1.24 ± 0.04	24.19 ± 0.21
F5	0.46 ± 0.04	0.62 ± 0.02	17.61 ± 0.04	1.25 ± 0.03	26.33 ± 0.22
F6	0.48 ± 0.04	0.64 ± 0.02	22.32 ± 0.03	1.31 ± 0.03	27.44 ± 0.21
F7	0.49 ± 0.03	0.61 ± 0.03	20.78 ± 0.03	1.27 ± 0.04	24.89 ± 0.18
F8	0.51 ± 0.03	0.55 ± 0.03	20.12 ± 0.02	1.20 ± 0.03	23.49 ± 0.11
F9	0.57 ± 0.03	0.68 ± 0.03	15.28 ± 0.02	1.18 ± 0.03	24.51 ± 0.23
F10	0.52 ± 0.02	0.62 ± 0.03	16.58 ± 0.02	1.21 ± 0.03	24.42 ± 0.21
F11	**0.50 ± 0.03**	**0.60 ± 0.02**	**18.90 ± 0.02**	**1.22 ± 0.03**	**25.10 ± 0.20**
F12	0.51 ± 0.04	0.59 ± 0.02	14.67 ± 0.04	1.20 ± 0.03	26.32 ± 0.22
F13	0.49 ± 0.04	0.61 ± 0.02	21.36 ± 0.03	1.27 ± 0.03	21.41 ± 0.21
F14	0.48 ± 0.03	0.60 ± 0.02	20.10 ± 0.02	1.23 ± 0.03	24.80 ± 0.20
F15	0.50 ± 0.03	0.63 ± 0.02	18.75 ± 0.03	1.19 ± 0.03	25.50 ± 0.18
F16	0.53 ± 0.02	0.64 ± 0.03	19.55 ± 0.02	1.22 ± 0.04	24.95 ± 0.19
F17	0.47 ± 0.03	0.61 ± 0.03	16.92 ± 0.03	1.26 ± 0.03	23.75 ± 0.22
F18	0.52 ± 0.03	0.62 ± 0.02	19.30 ± 0.03	1.21 ± 0.04	25.10 ± 0.21
F19	0.50 ± 0.04	0.59 ± 0.02	17.88 ± 0.04	1.24 ± 0.03	26.00 ± 0.22
F20	0.51 ± 0.04	0.60 ± 0.02	18.45 ± 0.03	1.22 ± 0.03	24.70 ± 0.21

Formulation of Capsule using optimized nanosponges

Of all the formulations, selected nanosponges (Nanosponges: F11) is added in hard gelatin capsule. These capsules had a theoretical Prednisolone content of 40mg. As a reference, capsules from a plain drug (i.e. without any polymer) are made to compare the dissolution behaviour of both the formulations as shown in Table 14, 15 and 16.

Tablet 14: Nanosponges Formulation

Sr. No.	Name of Ingredients	F11 Quantity
1	Nanosponges contain (Prednisolone:40mg; Eudragit S-100: 200mg; and PVA: 150mg)	390mg

Tablet 15: Capsule Formulation

Sr. No.	Name of Ingredients	F11 Quantity
1	Nanosponges equivalent (Prednisolone 40mg) for 1 Capsule	390mg
Total Weight	390mg	

Evaluation of Capsule

Table 16: Evaluation of Capsule containing nanosponges

Batch Code	Uniformity of Content	% Drug content
F11 Cap	0.1854 ± 0.03	98.25 ± 0.02

***In-vitro* dissolution**

The results of *in-vitro* dissolution study of capsules was performed in buffer pH 6.8 and showed that the formulation F11 containing showed ideal release of the drug in 12 hours as shown in Table 17 and Figure 12.

Table 17: *In-vitro* release profile of F11 Capsule

Sr. No.	Time (Hours)	F11 Cap
1	0	0
2	2	18.93±0.05
3	4	30.28±0.09
4	6	58.47±0.03
5	8	67.44±0.04
6	10	82.60±0.06
7	12	94.86±0.01

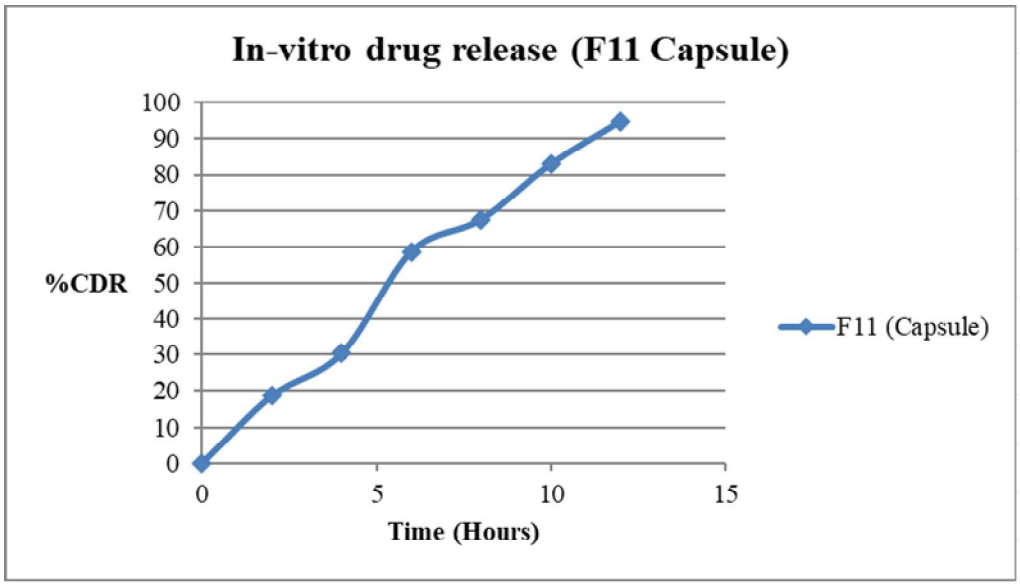

Figure 12: *In-vitro* drug release study F11 Capsule

Kinetics of drug release

The kinetics study of the F11 formulation was displayed in Table 18 and Figure 13 & 14. The data from *In Vitro* release of optimized formulations F11 were fit into various kinetic models to find out the mechanism of drug release from Prednisolone Nanosponges. A good linearity was observed with the zero order (R^2=0.9858), the zero-order kinetics explains the controlled release of the prepared Nanosponges over the period of 12 hours. Higuchi plot (R^2=0.9258) shows linearity, which indicates the rate of drug release through the mode of diffusion. Thus, the release kinetics of the optimized formulation was best fitted into Higuchi model and showed zero order drug release.

Table 18: R^2 values of various Kinetic Models

Kinetic Model	R^2 Value (F11 Cap)
Zero order release kinetics	0.9858
First order release kinetics	0.8976
Higuchi release kinetics	0.9258
Korsemeyer Peppas release kinetics	0.8723

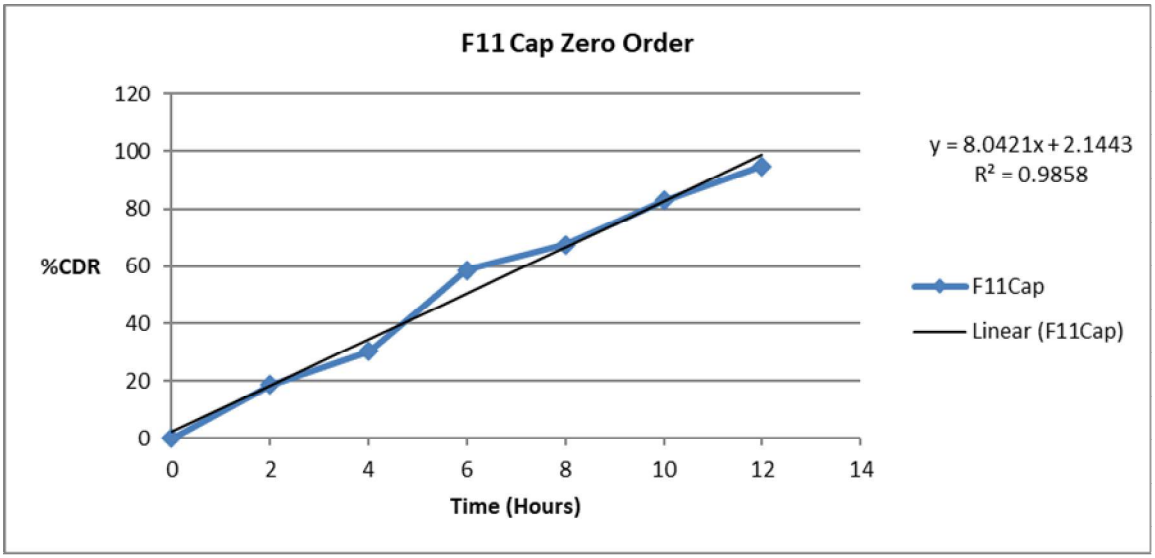

Figure 13: Kinetics of F11 Cap

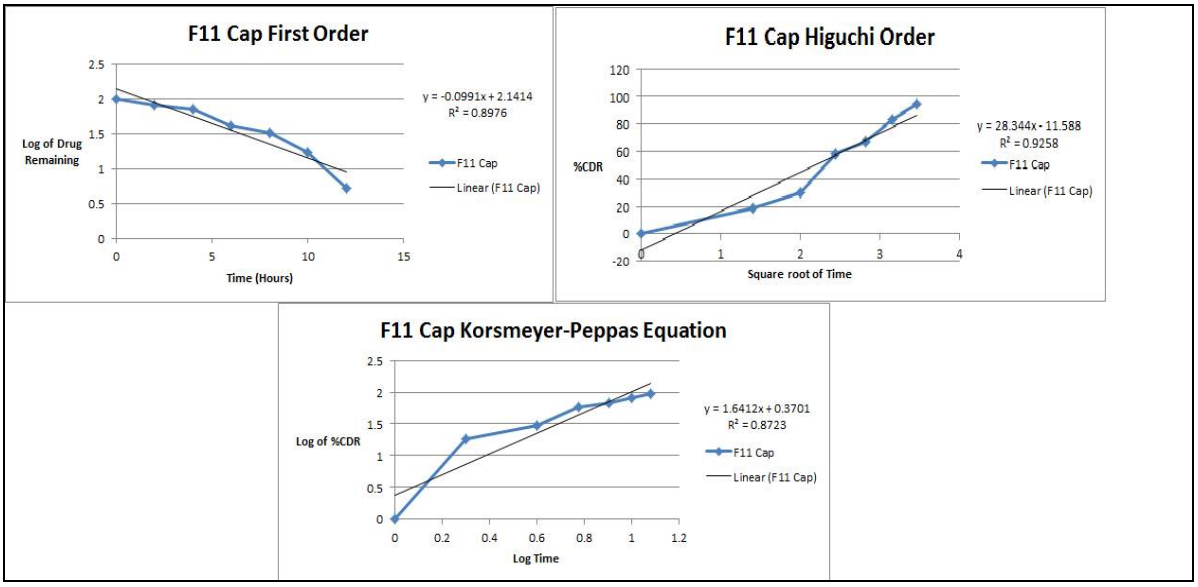

Figure 14: Kinetics of F11 Cap

Accelerated Stability Study

The optimized capsules were subjected to stability studies and the results are given in Table 19. Based on these results it is revealed that, capsule (Formulation batch F11) was found to be stable formulation at the given temperature and humidity condition.

Table 19: Stability study of parameters of the optimized formulation (F11)

Parameters	Initial Month	1st Month	2nd Month	3rd Month
Physical Appearance	No Change			
Drug Content	98.25±0.02	97.89 ± 0.03	97.45 ± 0.04	96.98 ± 0.05
Dissolution (%)	94.86±0.01	93.75 ± 0.02	92.68 ± 0.03	91.53 ± 0.04

CONCLUSION AND FUTURE DIRECTIONS

The optimized Prednisolone-loaded Eudragit S-100 nanosponges demonstrated favorable physicochemical properties, high entrapment efficiency, and sustained drug release following zero-order kinetics. The capsule formulation containing these nanosponges showed excellent drug content uniformity, controlled release for up to 12 hours, and satisfactory stability under accelerated storage conditions. The study confirmed that nanosponge-based systems could serve as an effective and promising platform for colon-targeted delivery of corticosteroids like Prednisolone. Future research should focus on *in vivo* pharmacokinetic and pharmacodynamic evaluations to correlate *In Vitro* release with therapeutic outcomes. Incorporating mucoadhesive or ligand-conjugated nanosponges may further enhance colonic retention and cellular uptake. Additionally, exploring biodegradable or stimuli-responsive polymers could enable on-demand drug release in response to the colonic microenvironment. The developed system offers a foundation for future translational research in site-specific delivery of anti-inflammatory agents for chronic gastrointestinal disorders.

REFERENCES

1. De Anda-Flores Y, Carvajal-Millan E, Campa-Mada A, Lizardi-Mendoza J, Rascon-Chu A, Tanori-Cordova J, et al. (2021). Polysaccharide-Based Nanoparticles for Colon-Targeted Drug Delivery Systems. Polysaccharides. 2(3):626–47.
2. Mathias H, Rohatinsky N, Murthy SK, Novak K, Kuenzig ME, Nguyen GC, et al. (2023). The 2023 Impact of Inflammatory Bowel Disease in Canada: Access to and Models of Care. J Can Assoc Gastroenterol. 6(2):S111–21.
3. Gupta JK, Singh AP, Sharma Y (2022). Exploring Chinese herbal medicine for the treatment of inflammatory bowel disease: A comprehensive overview. Pharmacol Res - Mod Chinese Med. 2024;10.
4. Iravani S, Varma RS. (2022). Nanosponges for Drug Delivery and Cancer Therapy: Recent Advances. Nanomaterials,. Vol. 12,
5. Al Refaai KA, AlSawaftah NA, Abuwatfa W, Husseini GA (2024). Drug Release via Ultrasound-Activated Nanocarriers for Cancer Treatment: A Review. Pharmaceutics. Vol. 16,
6. Sayed AH, Ramteke PP, Talware SR. (2025). Recent Advances in Computational Drug Delivery: From Nanoscale to Targeted Therapies.1(4):309–23.
7. Reji M, Kumar R. (2022). Response surface methodology (RSM): An overview to analyze multivariate data.

Indian Journal of Microbiology Research. Vol. 9. p. 241–8.
8. Veza I, Spraggon M, Fattah IMR, Idris M. (2023). Response surface methodology (RSM) for optimizing engine performance and emissions fueled with biofuel: Review of RSM for sustainability energy transition. Results in Engineering ,Vol. 18,
9. Jagadeesan S, Govindaraju I, Mazumder N. (2020). An Insight into the Ultrastructural and Physiochemical Characterization of Potato Starch: a Review. American Journal of Potato Research Vol. 97, p. 464–76.
10. Zhu WW, Zhao YF, Han ZZ, Wang XB, Wang YF, Liu G, et al. (2019). Thermal effect of different laying modes on cross-linked polyethylene (XLPE) insulation and a new estimation on cable ampacity. Energies;14(15).
11. Hani U, Al-Qahtani EH, Albeeshi FF, Alshahrani SS. (2025). Exploring the Landscape of Drug-Target Interactions: Molecular Mechanisms, Analytical Approaches, and Case Studies. J Pharm Sci Comput Chem.1(1):12–25.
12. Sversut RA, Alcântara IC, Rosa AM, Baroni ACM, Rodrigues PO, Singh AK, et al. (2017). Simultaneous determination of gatifloxacin and prednisolone acetate in ophthalmic formulation using first-order UV derivative spectroscopy. Arab J Chem.10(5):604–10.
13. Rogóż W, Owczarzy A, Kulig K, Maciążek-Jurczyk M. (2025). Ligand-human serum albumin analysis: the near-UV CD and UV-Vis spectroscopic studies. Naunyn Schmiedebergs Arch Pharmacol.398(3):3119–31.
14. Steiger M, (2019). Voigt W. Solid–Liquid Metastable Equilibria for Solar Evaporation of Brines and Solubility Determination: A Critical Discussion. J Solution Chem.48(7):1009–24.
15. Alotaibi BS, Khan MA, Ullah K, Yasin H, Mannan A, Khan SA, et al. (2024). Formulation and characterization of glipizide solid dosage form with enhanced solubility. PLoS One.19(2 February).
16. Siraj EA, Mulualem Y, Molla F, Yayehrad AT, Belete A. (2025). Formulation optimization of furosemide floating-bioadhesive matrix tablets using waste-derived Citrus aurantifolia peel pectin as a polymer. Sci Rep.15(1).
17. Das T, Patel DK. (2024). Efficient removal of cationic dyes using lemon peel-chitosan hydrogel composite: RSM-CCD optimization and adsorption studies. Int J Biol Macromol.275.
18. Tiwari K, Bhattacharya S. (2022). The ascension of nanosponges as a drug delivery carrier: preparation, characterization, and applications. J Mater Sci Mater Med.33(3).
19. Madhavi M, Shiva Kumar G. (2022). Preparation and Evaluation of Iguratimod Oral Formulation Using Cyclodextrin Nanosponges. Int J Appl Pharm.14(5):78–87.
20. Zhang H, Wu F, Li Y, Yang X, Huang J, Lv T, et al. (2016). Chitosan-based nanoparticles for improved anticancer efficacy and bioavailability of mifepristone. Beilstein J Nanotechnol.7:1861–70.
21. Kenechukwu FC, Kalu CF, Momoh MA, Onah IA, Attama AA, Okore VC. (2023). Novel Bos indicus Fat-Based Nanoparticulate Lipospheres of Miconazole Nitrate as Enhanced Mucoadhesive Therapy for Oral Candidiasis. Biointerface Res Appl Chem.13(1).
22. Maneerojpakdee D, Natapulwat N, Sinchaipanid N. (2025). Soybean Oil in Nifedipine-Loaded Nanostructured Lipid Carriers: Enhancing Drug Loading and Release. Pharm Sci Asia.52(2):240–9.
23. Caldera F, Nisticò R, Magnacca G, Matencio A, Monfared YK, Trotta F. (2022). Magnetic Composites of Dextrin-Based Carbonate Nanosponges and Iron Oxide Nanoparticles with Potential Application in Targeted Drug Delivery. Nanomaterials.12(5).
24. Jonas L, Jaksch H, Zellmann E, Klemm KI, Andersen PH. (2012). Detection of mercury in the 411-year-old beard hairs of the astronomer Tycho Brahe by elemental analysis in electron microscopy. Ultrastruct Pathol.36(5):312–9.
25. Shastri MA, Gadhave R, Talath S, Wali AF, Hani U, Puri S, et al. (2024). In silico Screening, Synthesis, and *In Vitro* Enzyme Assay of Some 1,2,3-Oxadiazole-linke Tetrahydropyrimidine-5-carboxylate Derivatives as DPP-IV Inhibitors for Treatment of T2DM. Chem Methodol.8(11):800–19.
26. Khan S, Pathan IK, Jamal R, Hudda S. (2025). Computational and *In Vitro* Exploration of Antioxidant and Anti-inflammatory Potential of Clitoria ternatea White-Flower Leaf Extract. Int J Biomed Investig.8(2):158–79.